Inorganic Chemistry
Article
Cite This: Inorg. Chem. XXXX, XXX, XXX−XXX
pubs.acs.org/IC

Selective Synthesis of Site-Differentiated Fe_4S_4 and Fe_6S_6 Clusters

Alex McSkimming and Daniel L. M. Suess*

Department of Chemistry, Massachusetts Institute of Technology, Cambridge, Massachusetts 02139, United States

Supporting Information

ABSTRACT: Obtaining rational control over the structure and nuclearity of metalloclusters is an ongoing challenge in synthetic Fe−S cluster chemistry. We report a new family of tridentate imidazolin-2-imine ligands $L(NIm^R)_3$ that can bind $[Fe_4S_4]^{2+}$ or $[Fe_6S_6]^{3+}$ clusters, depending on the steric profile of the ligand and the reaction stoichiometry. A high-yielding synthetic route to $L(NIm^R)_3$ ligands (where R is the imidazolyl N substituents) from trianiline and 2-chloroimidazolium precursors is described. For $L(NIm^{Me})_3$ (tris(1,3,5-(3-(*N*,*N*-dimethyl-4,5-diphenylimidazolin-2-imino)-phenylmethyl))benzene), metalation with 1 equiv of $[Ph_4P]_2[Fe_4S_4Cl_4]$ and 3 equiv of $NaBPh_4$ furnishes a mixture of products, but adjusting the stoichiometry to 1.5 equiv of $[Ph_4P]_2[Fe_4S_4Cl_4]$ provides $(L(NIm^{Me})_3)Fe_6S_6Cl_6$ in high yield. Formation of an $[Fe_6S_6]^{3+}$ cluster using $L(NIm^{Tol})_3$ (tris(1,3,5-(3-(*N*,*N*-bis(4-methylphenyl)-4,5-diphenylimidazolin-2-imino)phenylmethyl))-benzene) is not observed; instead, the $[Fe_4S_4]^{2+}$ cluster $[(L(NIm^{Tol})_3)(Fe_4S_4Cl)][BPh_4]$ is cleanly generated when 1 equiv of $[Ph_4P]_2[Fe_4S_4Cl_4]$ is employed. The selectivity for cluster nuclearity is rationalized by the orientation of the imidazolyl rings whereby long *N*-imidazolyl substituents preclude formation of $[Fe_6S_6]^{3+}$ clusters but not $[Fe_4S_4]^{2+}$ clusters. Thus, the structure and nuclearity of $L(NIm^R)_3$-bound Fe−S clusters may be selectively controlled through rational modification the ligand's substituents.

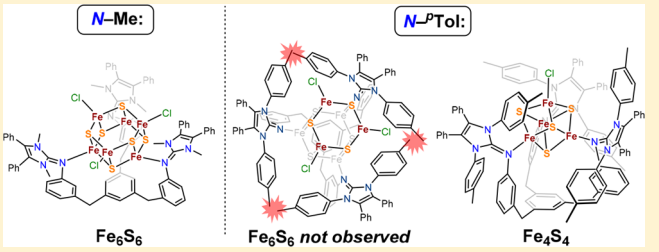

INTRODUCTION

Synthetic metal−chalcogenide clusters have been actively studied for decades owing to their applications in a number of diverse settings. For example, they serve as models for the active sites of Fe−S proteins,[1−3] as building blocks in nanomaterials,[4−7] and as catalysts in their own right.[8−17] Their broad utility in both biological and abiological contexts derives in part from the diversity of their geometric and electronic structures. Whereas nature has evolved complex biosynthetic pathways for controlling the structure and nuclearity of biological Fe−S clusters,[18−20] synthetic Fe−S clusters (as well as other metal−chalcogenide clusters) are often prepared through multicomponent self-assembly reactions that can be difficult to rationally control.[1−3,21,22] For example, the cuboidal cluster $[R_4E]_2[Fe_4S_4Cl_4]$ ($[R_4E]^+$ = $[Bu_4N]^+$ or $[Ph_4P]^+$) may be prepared from simple precursors (Scheme 1a).[23−25] Even a seemingly minor perturbation such as substitution of $[Bu_4N]^+$ or $[Ph_4P]^+$ by $[Et_4N]^+$ results in the generation of a cluster of different nuclearity, $[Et_4N]_3[Fe_6S_6Cl_6]$.[26,27] Moreover, the products of such self-assembly reactions can be subject to facile redistribution reactions. For example, $[Et_4N]_3[Fe_6S_6Cl_6]$ is itself thermally unstable and converts to $[Et_4N]_2[Fe_4S_4Cl_4]$ upon mild heating,[28] which, upon oxidation, undergoes a redistribution reaction to afford $[Et_4N]_2[Fe_6S_6Cl_6]$.[29] In addition, all-ferrous, phosphine-ligated Fe−S clusters readily rearrange to higher-nuclearity clusters: $Fe_4S_4(PR_3)_4$ clusters convert to $Fe_8S_8(PR_3)_6$ or $Fe_{16}S_{16}(PR_3)_8$ clusters depending on the phosphine substituents (Scheme 1, b), and as such the parent $Fe_4S_4(PR_3)_4$ clusters have not been isolated in analytically pure form.[30] Examples of rationally controlling the structure and nuclearity of Fe−S clusters are limited. Removal of the unique Fe from a site-differentiated Fe_4S_4 cluster bound to a chelating trithiolate ligand[31,32] allowed for the preparation of the first synthetic open-cuboidal Fe_3S_4 cluster;[33] much like a protein, this rigid scaffold prevents conversion to linear Fe_3S_4 clusters, which are favored in the absence of such a scaffold.[34,35]

Examples of rational synthetic cluster design are more abundant outside of Fe−S cluster chemistry. Betley et al. showed that a hexaamido ligand platform could support 3- or 6-Fe clusters depending on the metalation conditions (i.e., the identity of the Fe precursor and the presence or absence of additional phosphine ligands)[36,37] and that 8-Fe clusters could be accommodated by expanding the size of the ligand cavity and introducing an amine donor into the ligand framework.[38] In addition, reactive trimetallic clusters have been prepared using a rigid tris(diketiminate) scaffold developed by Murray et al.[39−42] and Agapie et al. have employed a ligand framework with three dipyridyl alkoxide groups anchored to a central phenyl group to selectively construct, for example, Mn_3O_4M (M = Ca^{2+}, Ln^{3+}, etc.) cubanes as models for the oxygen-evolving complex in photosystem II.[43−45]

We encountered challenges associated with controlling Fe−S cluster nuclearity in our efforts to generate site-differentiated Fe−S clusters using new donor sets. In particular, we targeted Fe−S clusters bound to tridentate, guanidine-like imidazolin-2-

Received: September 20, 2018

DOI: 10.1021/acs.inorgchem.8b02684
Inorg. Chem. XXXX, XXX, XXX−XXX

Scheme 1. Preparation of Fe−S Clusters of Variable Nuclearity[a]

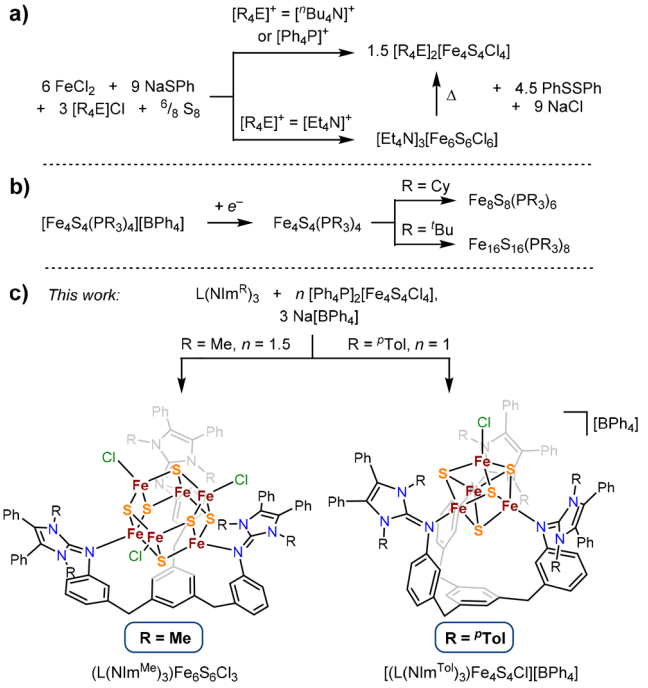

[a]Examples of (a and b) Fe−S core rearrangement reactions of synthetic clusters[28,30] and (c) rational control over cluster nuclearity presented in this work.

imines ligands $L(NIm^R)_3$ (Scheme 1c),[46−52] which we expected to be strongly binding, weak-field ligands that would mimic the donor properties of cysteine thiolates in proteins. We herein describe the synthesis of site-differentiated Fe−S clusters ligated by imidazolin-2-imines, demonstrate that the selectivity for cluster size may be rationally controlled by modifying the steric properties of the $L(NIm^R)_3$ ligands, and show that these ligands impart substantial steric protection to site-differentiated Fe_4S_4 clusters.

EXPERIMENTAL SECTION

General Methods. All manipulations involving metal complexes were carried out in an N_2 atmosphere glovebox. Glassware was oven-dried for at least several hours at 160 °C prior to use.

Spectroscopy and Spectrometry. NMR spectra were recorded on a Bruker 400 MHz spectrometer. ^1H and ^{13}C chemical shifts are reported in ppm relative to tetramethylsilane using residual solvent as an internal standard. Solution-phase effective magnetic moments were determined by the method described by Evans[53] and are corrected for diamagnetic contributions.[54] Zero-field ^{57}Fe Mössbauer spectra were measured with a constant acceleration spectrometer at 90 K. Isomer shifts are quoted relative to Fe foil at room temperature (RT). Data was analyzed and simulated with WMOSS v. 4.[55] Mass spectrometry data were collected on a JEOL AccuTOF spectrometer with a DART source or a Waters Q-TOF spectrometer with an ESI source. FTIR spectra were recorded on solid samples using a Bruker Alpha II FTIR Spectrometer operating at 2 cm^{-1} resolution. Elemental analysis were performed by Midwest Microlab.

X-ray Crystallography. X-ray intensity data were collected on a Bruker APEX CCD detector employing graphite-monochromated Mo Kα radiation (λ = 0.71073 Å) at 100(1) K. Absorption and other corrections were applied using SADABS.[56] The structures were solved by direct methods using SHELXT[57] and refined against F^2 on all data by full-matrix least-squares with SHELXL-2015.[58] Non-hydrogen atoms were refined anisotropically and hydrogen atoms were refined using a riding model.

Materials. THF was distilled from purple Na/benzophenone and distilled prior to use. Other solvents were sparged with argon and dried by passage through 2× columns packed with activated alumina. All solvents were stored over activated 3 Å molecular sieves for at least 24 h prior to use. All reagents were purchased from commercial suppliers and used without further purification unless otherwise noted. $[Ph_4P]_2[Fe_4S_4Cl_4]$,[25] *N,N*-dimethyl-4,5-diphenylimidazol-2-one,[59] and *N,N*-di(*p*-tolyl)-4,5-diphenylimidazol-2-one[60] were prepared according to literature procedures.

Synthesis of 1. 3-Nitroacetophenone (20.3 g, 0.123 mol) and dimethylformamide dimethyl acetal (29.3 g, 0.246 mol) were heated with stirring at 120 °C for 1 h. Excess solvent was removed under a stream of N_2 to afford a dark crystalline residue. Recrystallization from boiling methanol gave **1** as dark-orange crystals. Yield: 19.1 g (71%). Spectral data were consistent with that reported.[61]

Synthesis of 2. **1** (17.0 g, 0.0772 mol) was heated with stirring at vigorous reflux in acetic acid (80 mL) for 16 h. The reaction mixture was cooled to room temperature and ethanol (100 mL) was slowly added with rapid stirring to precipitate **2** as a yellow-brown solid. The product was collected on a frit, washed with ethanol until the washings were colorless, and dried under reduced pressure. Yield: 8.80 g, 65%. Spectral data were consistent with that reported.[62]

Synthesis of 3. **2** (5.00 g, 9.52 mmol) was suspended in methanol (50 mL) and the solution heated to boiling. $NaBH_4$ was added in ~200 mg portions until the solution became homogeneous (~1 g (26 mmol) required for complete conversion). ***Caution:*** *This reaction is exothermic with vigorous evolution of* H_2. The reaction mixture was cooled to room temperature, and water (500 mL) was added causing a brown oil to separate. After standing for 1 h the solvent was decanted, and the residue was taken up in diethyl ether (100 mL). The diethyl ether solution was washed with HCl (aqueous, 10%), washed with water, dried over sodium sulfate, and filtered through cotton wool. Removal of the solvent under reduced pressure gave a brown oil, which was extracted with several ~20 mL portions of diethyl ether. These were quickly filtered through a plug of cotton wool leaving a small amount of tarry brown residue. The solvent was removed thoroughly under reduced pressure to give an off white powder. Trituration with diethyl ether afforded **3** as a cream solid. Yield: 3.55 g, 71%. ^1H NMR (CD_3CN): δ 8.14 (t, J = 2.0 Hz, 3H, 3 × Ar*H*), 8.05 (dd, J = 8.0, 2.0 Hz, 3H, 3 × Ar*H*), 7.70 (d, J = 8.0 Hz, 3H, 3 × Ar*H*), 7.51 (t, J = 8.0 Hz, 3H, 3 × Ar*H*), 7.35 (s, 3H, 3 × Ar*H*), 5.86 (d, J = 3.4 Hz, 3H, C*H*OH), 4.17 (d, J = 3.4 Hz, 3H, O*H*). $^{13}C\{^1H\}$ NMR (CD_3CN): 149.23, 147.94, 145.71, 133.55, 130.51, 124.68, 122.97, 121.71 (8 × ArC), 74.75 (*C*OH). DART-MS (+): m/z 514.1235; calcd for $[M - OH]^+$: m/z 514.1256.

Synthesis of 4. **3** (3.00 g, 5.69 mmol) was suspended in dichloromethane (50 mL) and triethylsilane (3.6 mL, 22.5 mmol), then $BF_3{\cdot}Et_2O$ (2.9 mL, 23.1 mmol) added with stirring. Stirring was continued at room temperature for 24 h at which point the reaction mixture was nearly homogeneous. The reaction mixture was filtered through a pad of Celite, transferred to a separatory funnel and washed with water (50 mL). The organic layer was dried over sodium sulfate and passed through a short (~5 cm) pad of silica. The silica was washed with dichloromethane until the product had fully eluted (as determined by TLC; CH_2Cl_2, R_f ~0.6). Solvent was removed under reduced pressure and the residue recrystallized from dichloromethane-ethanol to afford **4** as pale yellow crystals. Although minor impurities were visible by NMR spectroscopy, this material was sufficiently pure for the next step. Yield: 2.45 g (89%). ^1H NMR ($CDCl_3$): δ 8.05 (d, J = 7.6 Hz, 3H, 3 × Ar*H*), 7.99 (s, 3H, 3 × Ar*H*), 7.48 (d, J = 7.6 Hz, 3H, 3 × Ar*H*), 7.45 (t, J = 7.6 Hz, 3H, 3 × Ar*H*), 6.89 (s, 3H, 3 × Ar*H*), 4.03 (s, 6H, CH_2). $^{13}C\{^1H\}$ NMR ($CDCl_3$): δ 148.53, 142.84, 140.74, 135.14, 129.60, 128.16, 123.72, 121.60 (8 × ArC), 41.33 (CH_2). DART-MS (+): m/z 484.1502; calcd for $[M + H]^+$: m/z 484.1509.

Synthesis of 5. **4** (2.00 g, 4.17 mmol) was suspended in THF (30 mL) and heated to 70 °C with stirring until the mixture became homogeneous. Solid ammonium formate (~6 g, ~100 mmol) was added followed by absolute ethanol (30 mL). The mixture was heated

DOI: 10.1021/acs.inorgchem.8b02684
Inorg. Chem. XXXX, XXX, XXX−XXX

to 80 °C and Pd/C (5%, ∼100 mg) added cautiously (vigorous gas evolution). The reaction mixture was maintained at 80 °C until the reaction was complete (as determined by TLC; EtOAc-Et_2O (1:3), R_f ∼0.4), cooled to room temperature, and filtered through a pad of Celite. The solution was diluted with water (200 mL) and diethyl ether (50 mL). The organic layer was separated and washed with 3 × 50 mL portions of water. The organic layer was dried over sodium sulfate and passed through a ∼5 cm pad of silica, which was washed with diethyl ether until all of the product had eluted (as determined by TLC). The solvent was removed under reduced pressure and the residue recrystallized from dichloromethane-hexanes to afford **5** as a white crystalline solid. Yield: 1.41 g (86%). ^{1}H NMR (CD_3CN): δ 6.97 (t, J = 7.6 Hz, 3H, 3 × Ar*H*), 6.90 (s, 3H, 3 × Ar*H*), 6.45 (m, 9H, 9 × Ar*H*), 4.04 (s, br, 6H, NH_2), 3.73 (s, 6H, CH_2). ^{13}C{^{1}H} NMR (CD_3CN): δ 148.95, 143.41, 142.80, 130.03, 127.85, 118.60, 115.65, 113.10 (8 × Ar*C*), 42.34 (*C*H_2). DART-MS (+): m/z 394.2288; calcd for $[M + H]^+$: m/z 394.2283.

Synthesis of 6. 1,2-Dimethyl-4,5-diphenylimidazol-2-one (15.1 g, 0.0571 mol) was heated in $POCl_3$ (30 mL) at 110 °C for 16 h. Excess $POCl_3$ was distilled from the reaction mixture to yield a pale blue oil which was dissolved in methanol (∼50 mL). To this solution was slowly added a saturated aqueous solution of KPF_6 (∼100 mL), which caused a white solid to precipitate. Additional water (∼300 mL) was added to the mixture, and the solid was collected by filtration, washed with copious water, and dried under reduced pressure. Recrystallization from acetone−isopropanol afforded **6** as colorless crystals. Yield: 14.8 g, 61%. ^{1}H NMR (CD_3CN): δ 7.44−7.53 (m, 6H, 6 × Ar*H*), 7.35−7.37 (m, 4H, 4 × Ar*H*), 3.64 (s, 6H, 2 × N−CH_3). ^{13}C{^{1}H} NMR (CD_3CN): δ 133.42 (*C*−Cl), 132.97, 131.72, 131.52, 130.01, 125.90 (5 × Ar*C*), 34.68 (N−CH_3). ^{31}P NMR (CD_3CN): δ −144.6 (sept, J_{PF} = 712 Hz, [*P*F_6]$^-$). DART-MS (+): m/z 283.0997; calcd for $[M]^+$: m/z 283.1002.

Synthesis of 7. 1,2-Di(*p*-tolyl)-4,5-diphenylimidazol-2-one (4.00 g, 9.60 mmol) was heated in $POCl_3$ (8 mL) at 110 °C for 16 h. Excess $POCl_3$ was distilled from the reaction mixture to yield a pale yellow oil, which was dissolved in methanol (∼20 mL). To this solution was slowly added a saturated aqueous solution of KPF_6 (∼20 mL), which caused a white solid to precipitate. Additional water (∼200 mL) was added to the mixture and the solid collected by filtration, washed with copious water, and dried under reduced pressure. Recrystallization from dichloromethane−isopropanol afforded **7** as colorless crystals. Yield: 4.95 g, 89%. ^{1}H NMR (CD_3CN): δ 7.45 (d, J = 8.2 Hz, 4H, 4 × Ar*H*), 7.36 (d, J = 8.2 Hz, 4H, 4 × Ar*H*), 7.24−6.34 (m, 10H, 10 × Ar*H*), 2.38 (s, 6H, 2 × Ar−CH_3). ^{13}C{^{1}H} NMR (CD_3CN): δ 143.07 (*C*−Cl), 134.42, 134.31, 132.00, 131.48, 131.22, 130.97, 129.57, 128.31, 125.98 (9 × Ar*C*), 21.24 (Ar−CH_3). ^{31}P NMR (CD_3CN): δ −144.6 (sept, J_{PF} = 712 Hz, [*P*F_6]$^-$). DART-MS (+): m/z 435.1632; calcd for $[M]^+$: m/z 435.1625.

Synthesis of L(NIm^{Me})$_3$ (8). In a glovebox, a solution of LiHMDS (603 mg, 3.60 mmol) in THF (2 mL) was cooled to −35 °C and added dropwise with stirring to a cold (−35 °C) suspension of **5** (215 mg, 0.546 mmol) and **6** (738 mg, 1.72 mmol) in THF (6 mL). The mixture was allowed to come to RT and stirred for a further 1 h to give an orange solution. The following operations were performed in air. The solvent was removed under reduced pressure to give an orange oil, which was partitioned between water (∼2 mL) and benzene (5 mL). The organic layer was separated, dried over sodium sulfate, and filtered, and the solvent was removed under reduced pressure. The oily residue was dissolved in boiling acetonitrile (5 mL), then cooled to −10 °C to induce separation of a yellow oil. The orange supernatant was decanted and the residue was dried thoroughly under reduced pressure. Trituration with hexanes gave the product as a pale yellow powder. Yield: 571 mg, 92%. ^{1}H NMR (C_6D_6): δ 7.08−7.15 (m, 9H, 9 × Ar*H*), 6.75−7.02 (m, 33H, 33 × Ar*H*), 6.75 (d, J = 7.2 Hz, 3H, 3 × Ar*H*), 3.89 (s, 6H, 3 × CH_2), 2.85 (s, 18H, 3 × N−CH_3). ^{13}C{^{1}H} NMR (C_6D_6) δ 151.93 (*C*═N), 149.25, 142.59, 142.01, 130.05, 129.84, 129.14, 128.80, 124.32, 121.97, 120.15, 119.59 (11 × Ar*C*; 2 × concealed by C_6D_6 resonances), 42.78 (*C*H_2), 32.53 (N−*C*H_3). FTIR: cm^{-1} 3051w, 2919w, 1615m, 1564s, 1503w, 1481w, 1452m, 1420m, 1377m, 1318w, 1230w, 1178w, 1155w, 1072w, 1040w, 1020m, 994w, 917w, 885w, 864w, 841w, 790w, 763w, 743w, 696s, 651w, 599w, 505w, 449w. ESI-MS (+): m/z 1132.5736; calcd for $[M + H]^+$: m/z 1132.5754.

Synthesis of L(NIm^{Tol})$_3$ (9). In a glovebox, a solution of LiHMDS (584 mg, 3.49 mmol) in THF was cooled to −35 °C and added dropwise with stirring to a cold (−35 °C) suspension of **5** (208 mg, 0.529 mmol) and **7** (968 mg, 1.67 mmol) in THF (10 mL). The mixture was allowed to come to RT and stirred for a further 1 h to give a yellow solution. The following operations were performed in air. The solvent was removed under reduced pressure to give a yellow solid, which was partitioned between water (∼2 mL) and benzene (5 mL). The organic layer was separated, dried over sodium sulfate, and filtered, and the solvent removed under reduced pressure. The oily residue was dissolved in dichloromethane (∼1 mL) and diluted with acetonitrile (20 mL), and the solution was concentrated to ∼10 mL, which caused the product to separate as a flocculent, pale-yellow solid. This solid was collected by filtration, washed with acetonitrile (3 × 5 mL), and dried under reduced pressure. Yield: 756 mg, 90%. ^{1}H NMR (C_6D_6): δ 7.85 (d, J = 8.2 Hz, 12H, 12 × Ar*H*), 7.07 (d, J = 8.2 Hz, 12H, 12 × Ar*H*), 6.98 (s, 3H, 3 × Ar*H*), 6.78−6.87 (m, 21H, 21 × Ar*H*), 6.64−6.66 (m, 18H, 18 × Ar*H*), 6.49 (d, J = 7.4 Hz, 3H, 3 × Ar*H*), 3.61 (s, 6H, 3 × CH_2), 1.91 (s, 18H, 6 × Ar−CH_3). ^{13}C{^{1}H} NMR (C_6D_6): δ 150.17 (C═N), 144.85, 141.85, 140.88, 136.27, 135.17, 130.89, 130.17, 129.08, 128.97, 127.54, 124.38, 123.54, 120.61, 119.83 (15 × Ar*C*; 2 × concealed by C_6D_6 resonances), 42.40 (*C*H_2), 20.98 (Ar−*C*H_3). FTIR: cm^{-1} 3032w, 2920w, 1651s, 1586s, 1575s, 1513s, 1502m, 1482w, 1445m, 1375s, 1313w, 1279w, 1239m, 1211w, 1177w, 1160w, 1106m, 1073w, 1033w, 1021w, 982w, 960w, 937w, 916w, 889w, 809m, 794m, 760m, 735w, 722w, 695s, 638w, 615w, 587w, 536m, 523m, 506w, 491w, 476w, 456w, 444w. ESI-MS (+): m/z 1588.7614; calcd for $[M + H]^+$: m/z 1588.7632.

Synthesis of (L(NIm^{Me})$_3$)Fe$_6$S$_6$Cl$_3$ (11). To a stirred suspension of $NaBPh_4$ (385 mg, 1.13 mmol) in dichloromethane (3 mL) was rapidly added a solution of L(NIm^{Me})$_3$ (411 mg, 0.363 mmol) and [Ph_4P]$_2$[$Fe_4S_4Cl_4$] (639 mg, 0.545 mmol) in dichloromethane (6 mL). Stirring was continued for 2 h. The dark-crimson reaction mixture was then filtered through a pad of Celite. Solvent was removed under reduced pressure and the crude solid was washed with acetonitrile (5 × 2 mL) to afford the complex as black-red microcrystals (545 mg, 85%). Crystals suitable for XRD studies were grown by layering a THF solution with hexanes. Elemental analysis was conducted on a sample recrystallized from toluene−acetonitrile. Evans method ($CDCl_3$): 3.6 μ_B. UV−vis (THF): λ_{max} (nm) ε_{max} (M^{-1} cm^{-1}) 348 (sh, 2.3 × 10^4), 496 (1.7 × 10^4). ^{1}H NMR ($CDCl_3$): δ 10.32 (t (partially resolved), J = 7 Hz, 3H, 3 × 5-^{bridge}Ph*H*), 7.46 (12H, 12 × Ar*H*), 7.28 (6H, 6 × Ar*H*), 7.07 (12H, 12 × Ar*H*), 7.02 (s, 3H, 3 × ^{basal}Ph*H*), 5.46 (s, 18H, 3 × N−CH_3), 4.55 (3H, 3 × 2-^{bridge}Ph*H*), 2.38 (d (partially resolved), J = 7 Hz, 3H, 3 × 4/6-^{bridge}Ph*H*), 2.12 (s, 6H, 3 × CH_2), 2.00 (d, J = 7.3 Hz, 3H, 3 × 4/6-^{bridge}Ph*H*). ^{13}C{^{1}H} NMR ($CDCl_3$) δ 213.93, 208.69, 191.65, 162.28, 154.10, 138.47, 136.45, 131.64, 130.55, 130.44, 128.62, 125.00, 121.93, 118.87 (14 × Ar*C*), 46.42 (*C*H_2), 29.43 (N−*C*H_3). FTIR: cm^{-1} 3052w, 2948w, 2899w, 1601m, 1573m, 1517s, 1482s, 1441s, 1418m, 1359w, 1290m, 1228m, 1156m, 1090w, 1076w, 1053w, 1043w, 1023w, 997w, 971w, 920w, 874m, 854m, 809w, 764s, 733w, 721w, 699s, 616w, 597w, 549w, 509w. Elemental analysis for $C_{78}H_{69}Cl_3Fe_6N_9S_6$·1.5$C_7H_8$·$CH_3CN$: calcd C, 55.87; H, 4.35; N, 7.30. Found C, 56.24; H, 4.32; N, 7.23.

Synthesis of [(L(NIm^{Tol})$_3$)(Fe$_4$S$_4$Cl)][BPh$_4$] (12). To a stirred suspension of L(NIm^{Tol})$_3$ (414 mg, 0.261 mmol) and [Ph_4P]$_2$[$Fe_4S_4Cl_4$] (306 mg, 0.261 mmol) in THF (5 mL) was added a solution of $NaBPh_4$ (277 mg, 0.809 mmol) in THF (3 mL) dropwise. Stirring was continued for 2 h. The orange-brown reaction mixture was filtered through a pad of Celite. Solvent was removed under reduced pressure and the crude solid washed with MeCN (3 × 2 mL) then diethyl ether (3 × 5 mL) to afford the complex as dark-brown microcrystals (478 mg, 80%). Crystals suitable for XRD studies were grown by layering a chloroform solution with hexanes. Elemental analysis was conducted on a sample recrystallized from from CH_2Cl_2−hexanes. Evans method ($CDCl_3$): 2.7 μ_B. UV−vis (THF): λ_{max} (nm) ε_{max} (M^{-1} cm^{-1}) 468 (1.1 × 10^4), 736 (sh, 2.0 × 10^3). ^{1}H NMR ($CDCl_3$): δ 8.15 (3H, 3 × 5-^{bridge}Ph*H*), 7.48 (m, 8H, 8 × *o*-Ph*H*$_4$B),

DOI: 10.1021/acs.inorgchem.8b02684
Inorg. Chem. XXXX, XXX, XXX−XXX

Scheme 2. Synthesis of Ligands L(NIm^{Me})$_3$ (8) and L(NIm^{Tol})$_3$ (9)

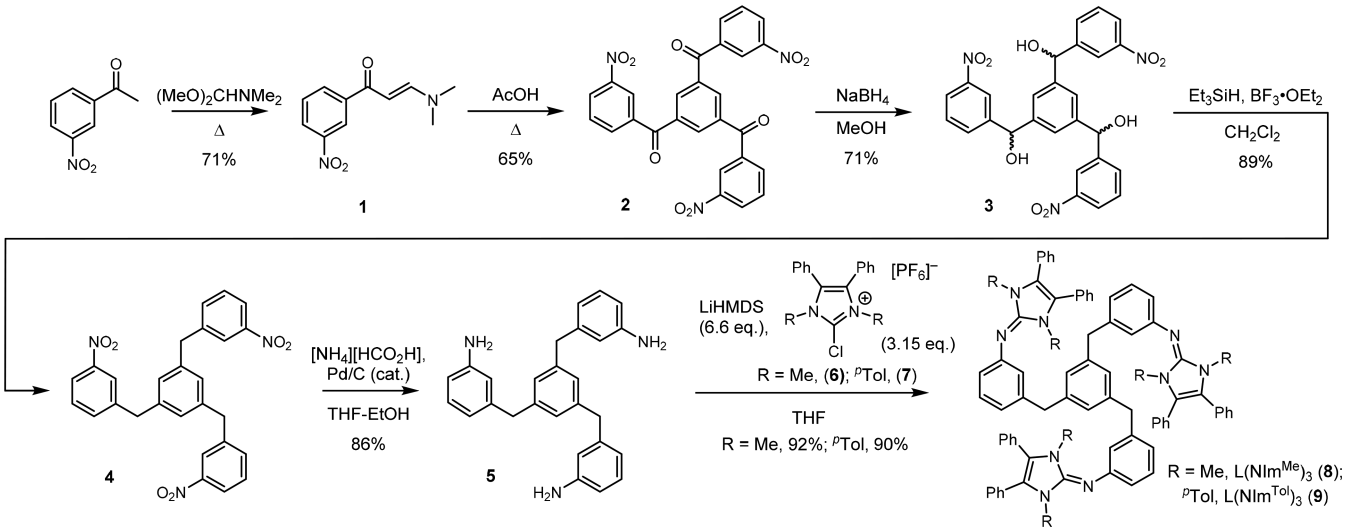

7.16 (20H, 20 × Ar*H*), 7.08 (t, *J* = 7.1 Hz, 8H, 8 × *m*-Ph*H*$_4$B), 6.96 (17H, 17 × Ar*H*), 6.90 (t, *J* = 7.1 Hz, 4H, 4 × *p*-Ph*H*$_4$B), 6.75 (12H, 12 × Ar*H*), 5.98 (3H, 3 × ^{basal}Ph*H*), 5.60 (3H, 3 × 4/6-^{bridge}Ph*H*), 5.38 (3H, 3 × 4/6-^{bridge}Ph*H*), 3.55 (3H, 3 × 2-^{bridge}Ph*H*), 3.01 (s, 6H, 3 × C*H*$_2$), 2.28 (s, 18H, 3 × Ar−C*H*$_3$). ^{13}C NMR (126 MHz, CDCl$_3$) *δ* 169.86 (br, ArC), 166.85 (br, ArC), 164.98 (br, ArC), 164.53 (q, J_{BC} = 40 Hz, ^{ipso}C−BPh$_4$), 150.59 (ArC), 140.67 (ArC), 139.58 (ArC), 136.51 (^{meta}C−BPh$_4$), 135.19 (ArC), 134.67 (ArC), 132.48 (br, ArC), 132.21 (ArC), 130.29 (ArC), 129.52 (ArC), 128.61 (ArC), 128.56 (ArC), 128.45 (br, ArC), 125.65 (ArC), 125.57 (q, J_{BC} = 21 Hz, ^{ortho}C−BPh$_4$), 125.52 (ArC), 121.63 (^{para}C−BPh$_4$), 43.41 (*C*H$_2$), 21.69 (Ar−*C*H$_3$); 1 × ArC not observed. FTIR: cm^{-1} 3053w, 3031w, 2981w, 2917w, 1600w, 1575w, 1515m, 1479s, 1447m, 1422s, 1377w, 1309w, 1264w, 1227w, 1179w, 1158w, 1114w, 1088w, 1072w, 1031w, 1019w, 999w, 958w, 916w, 868w, 817m, 791w, 782w, 731m, 696s, 678s, 639w, 611m, 574w, 534m, 523m, 494w, 475w, 475w. Elemental analysis for C$_{138}$H$_{113}$BClFe$_4$N$_9$S$_4$·2CH$_2$Cl$_2$: calcd C, 68.21; H, 4.78; N, 5.11. Found C, 68.24; H, 4.99; N, 4.78.

RESULTS

The tridentate L(NIm^R)$_3$ ligands employed in this work adopt the general geometry imposed by Holm's seminal, site-differentiating trithiolate ligand,[31,32] analogs of which have been fruitfully employed by other research groups.[63−65] The new ligands presented in this work were prepared as shown in Scheme 2. First, condensation of 3-nitroacetophenone with *N*,*N*-dimethylformamide dimethyl acetal followed by thermal cyclization of resulting enone **1** provided trinitrotrione **2**. Stepwise reduction of the nitro and ketone groups furnishes trianiline **5**,which can be readily prepared on a multigram scale. Trianiline **5** may be reacted with a variety of 2-chloroimidazoliums in the presence of strong base to furnish ligands including L(NIm^{Me})$_3$ (**8**) and L(NIm^{Tol})$_3$ (**9**) in >90% yield; **5** is therefore a useful precursor for introducing different imidazolyl groups in the final synthetic stages.

Attempts to prepare an L(NIm^{Me})$_3$-ligated [Fe$_4$S$_4$]$^{2+}$ cluster by metalation of L(NIm^{Me})$_3$ with 1 equiv of [Ph$_4$P]$_2$[Fe$_4$S$_4$Cl$_4$] and 3 equiv of NaBPh$_4$ resulted in a mixture of species including [(L(NIm^{Me})$_3$)Fe$_4$S$_4$Cl][BPh$_4$] (**10**) and the higher-nuclearity cluster (L(NIm^{Me})$_3$)Fe$_6$S$_6$Cl$_3$ (**11**) in a roughly 4:1 ratio (Scheme 3 and Figure S26). Cationic cluster **10** could not be isolated but was identified by comparison with the ^{1}H NMR spectrum of [(L(NIm^{Tol})$_3$)Fe$_4$S$_4$Cl][BPh$_4$] (*vide infra*). Complex **11** could be cleanly generated by appropriately adjusting

Scheme 3. Metalation Reactions of L(NIm^R)$_3$ Presented in This Work

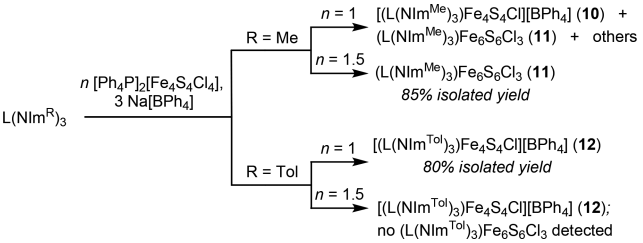

the reaction stoichiometry (i.e., using 1.5 equiv of [Ph$_4$P]$_2$[Fe$_4$S$_4$Cl$_4$]). Unlike [Et$_4$N]$_3$[Fe$_6$S$_6$Cl$_6$], complex **11** is thermally stable (as a CDCl$_3$ solution at 60 °C over 24 h.).

The ^{1}H NMR spectrum of **11** (Figure 1) shows paramagnetically shifted resonances, the most dramatically affected being those for the ^{1}H nuclei on the phenylene group directly bound to the N donor (*δ* 10.32, 4.55, 2.38, and 2.00), which were identified by a ^{1}H−^{1}H COSY experiment (Figure S17). At RT, **11** displays C_{3v} symmetry on the NMR time scale (400 MHz). The ground spin state is $S = {}^1/_2$ as shown by its EPR spectrum (Figure S24), which resembles that of other known [Fe$_6$S$_6$]$^{3+}$ clusters.[28] The zero-field ^{57}Fe Mössbauer spectrum of solid **11** (Figure 3a) shows two quadrupole doublets in a 1:1 ratio with isomer shifts of 0.46 and 0.52 mm s^{-1} (ΔE_Q = 0.89 and 1.25 mm s^{-1}, respectively), consistent with two chemically distinct sets of three Fe centers (one set Cl ligated, the other NIm ligated). The Mössbauer parameters for **11** are similar to those reported for [Fe$_6$S$_6$X$_6$]$^{3-}$ clusters (X = halide, RS$^-$, RO$^-$; e.g., X = Cl, *δ* = 0.50 mm s^{-1}, ΔE_Q = 1.08 mm s^{-1}), suggesting a similar electronic structure in which charge is delocalized over the six Fe sites to give an average Fe oxidation state of +2.5.[28]

The molecular structure of **11** determined by X-ray crystallography (Figure 3, a) shows a distorted hexagonal prismane geometry for the Fe−S cluster akin to that of other reported [Fe$_6$S$_6$]$^{3+}$ complexes.[26−28,66] The L(NIm^{Me})$_3$ ligand binds three Fe centers on one face of the prismane with an average Fe−N distance of 1.98 Å. This is somewhat shorter than those reported for NIm-ligated, tetrahedral high-spin Fe^{2+} complexes (2.05 Å avg),[67] likely a result of the effective Fe oxidation state of +2.5 (*vide supra*), which results in a slight

DOI: 10.1021/acs.inorgchem.8b02684
Inorg. Chem. XXXX, XXX, XXX−XXX

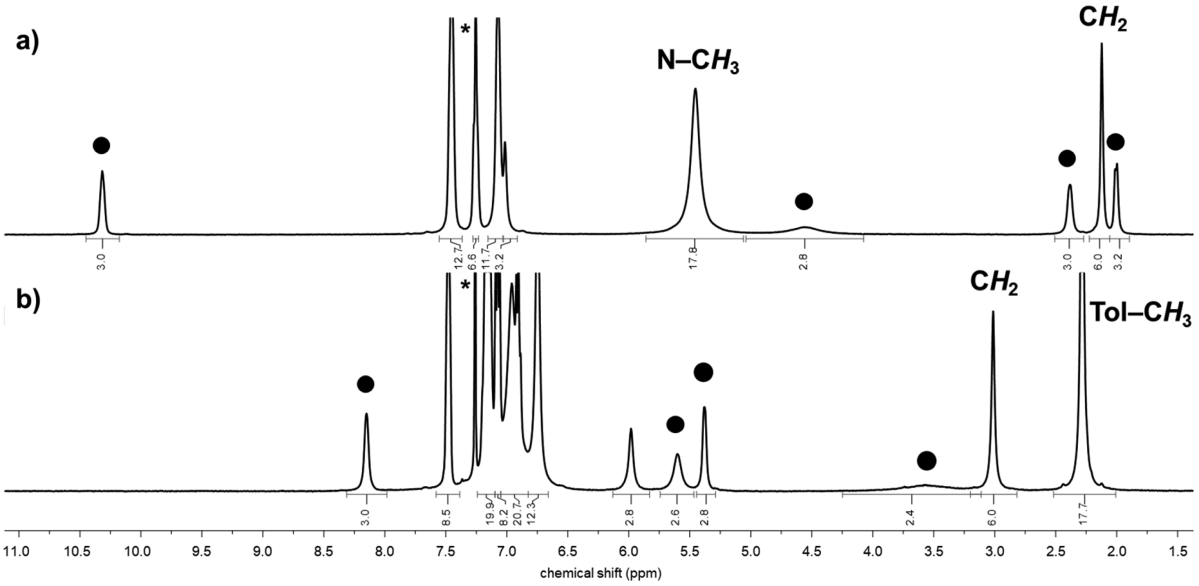

Figure 1. ^{1}H NMR spectra of (a) $(L(NIm^{Me})_3)Fe_6S_6Cl_3$ and (b) $[(L(NIm^{Tol})_3)Fe_4S_4Cl][BPh_4]$ recorded in $CDCl_3$ at 400 MHz. Peaks marked with circles were assigned to the bridge-phenylene protons. Asterisks mark the peak due to $CDCl_3$.

contraction of the Fe–N bonds. The average interdonor N–N distance is 6.86 Å, indicative of splaying of the ligand arms away from the basal phenyl ring compared with $[(L(NIm^{Tol})_3)Fe_4S_4Cl][BPh_4]$ (*vide infra*). The imidazolyl rings are positioned nearly upright with respect to the molecular 3-fold rotational axis ($\angle(S_{axial}–Fe–N–C_{imid}) \approx 9°$ (avg) where the S_{axial}–Fe bond is parallel to the molecular pseudo-C_3 axis; see Figures 3a and 4a).

On the basis of the structure of **11** and some computational modeling, we made several predictions relevant to achieving clean synthetic access to Fe_4S_4 clusters bound to $L(NIm^R)_3$ ligands: First, that $L(NIm^R)_3$ ligands based on this tri(arylmethyl)aryl framework should also accommodate Fe_4S_4 clusters; second, and most importantly, that unlike for the Fe_6S_6 cluster **11**, the imidazolyl rings in $L(NIm^R)_3$-bound Fe_4S_4 clusters would be substantially tilted with respect to the molecule's pseudo-3-fold rotational axis. Thus, we predicted that the substituents on the imidazolyl N atoms would determine the ability of $L(NIm^R)_3$ ligands to accommodate an Fe_6S_6 cluster: Although shorter substituents (e.g., methyl in $L(NIm^{Me})_3$) clearly allow for Fe_6S_6 cluster binding, longer substituents (e.g., *p*-tolyl in $L(NIm^{Tol})_3$) would clash with neighboring substituents and disfavor Fe_6S_6 cluster formation (Figure 4a). However, longer substituents should be tolerated in $L(NIm^{Tol})_3$-bound Fe_4S_4 clusters owing to the tilt of the imidazolyl rings, which allows for the donor arms to pack more tightly around the Fe_4S_4 cluster (Figure 4b).

To test these hypotheses, we metalated $L(NIm^{Tol})_3$ with 1 equiv of $[Ph_4P]_2[Fe_4S_4Cl_4]$ and 3 equiv of $NaBPh_4$, which resulted in clean formation of the desired complex $[(L(NIm^{Tol})_3)Fe_4S_4Cl][BPh_4]$ (**12**)(Scheme 3). Under no conditions have we been able to generate an Fe_6S_6 cluster of $L(NIm^{Tol})_3$ (for example, by adjusting the stoichiometry to use 1.5 equiv of $[Ph_4P]_2[Fe_4S_4Cl_4]$ (Figure S26) or heating **12** in the presence of 0.5 equiv of $[Ph_4P]_2[Fe_4S_4Cl_4]$). Thus, through simple and rational modification of the steric profile of the $L(NIm^R)_3$ ligand, site-differentiated $[Fe_4S_4]^{2+}$ or $[Fe_6S_6Cl_3]^{3+}$ clusters may be generated with high selectivity.

Like complex **11**, complex **12** displays C_{3v} symmetry on the NMR time scale (400 MHz) at RT (Figure 1). The ^{1}H resonances attributed to the donor-N aryl rings (δ 8.15, 6.60, 5.38 and 3.55) are less dramatically shifted compared with those of **11** owing to the diamagnetic ground state of **12**.[1,68,68] However, they are somewhat shifted owing to the population of paramagnetic excited states; the RT solution magnetic moment determined by the Evans method (2.7 μ_B) is consistent with this proposal and with those of other $[Fe_4S_4]^{2+}$ clusters.[1,68,69] The zero-field ^{57}Fe Mössbauer spectrum of solid **12** was best simulated as two quadrupole doublets in a 3:1 ratio of roughly the same isomer shift (0.48 mm s^{-1}), reflecting both (i) the distinct coordination environment of the apical Fe center[70,71] and (ii) charge delocalization over the four Fe sites resulting in effective Fe oxidations state of +2.5.[1,72–75]

The structure of **12** shows the anticipated ligand binding mode with three Fe atoms bound by $L(NIm^{Tol})_3$ and the unique Fe atom bound by Cl (Figure 3b). As anticipated, the imidazolyl rings are significantly tilted ($\angle(S_{basal}–Fe–N{=}C_{imid}) \approx 50°$ (avg) where S_{basal} is located on the pseudo-C_3 axis; see Figures 3b and 4b), thereby allowing the sterically demanding *p*-tolyl groups to fit around the cluster core. The dramatic descent in symmetry from solution (C_{3v}) to the solid state (C_3) indicates that in solution the imidazolyl rings are rapidly flipping about the pseudo σ_v planes. The Fe–N distances in **12** are similar to those for **11** (1.98 Å, avg). The average interdonor N–N distance in **12** (5.93 Å) is ~15% shorter than that in **11** as accommodation of the smaller cluster core requires less splaying of the ligand arms.

DISCUSSION

The encapsulation of clusters of specific nuclearity in chelating ligands presents additional challenges compared with binding chelating ligands to mononuclear metal sites. Clusters require larger ligands that typically have more degrees of freedom. As such, multiple small twists in the dihedral angles of the ligand backbone can cumulatively lead to a broad distribution of possible interdonor distances and orientations, which can lead to a binding pocket that accommodates a number of cluster structures. This challenge is illustrated by the ability of the $L(NIm^{Me})_3$ ligand to bind both $[Fe_4S_4]^{2+}$ and $[Fe_6S_6]^{3+}$ clusters

DOI: 10.1021/acs.inorgchem.8b02684
Inorg. Chem. XXXX, XXX, XXX–XXX

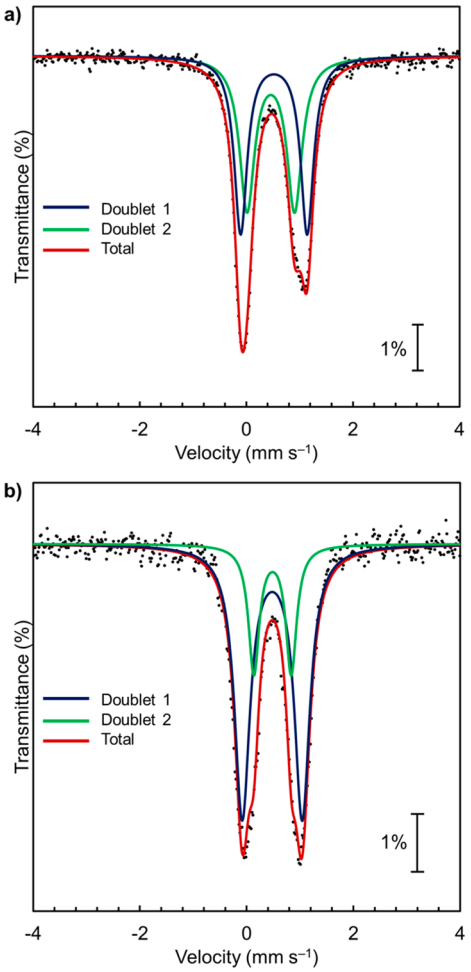

Figure 2. Zero-field ^{57}Fe Mössbauer spectra of solid (a) $(L(NIm^{Me})_3)Fe_6S_6Cl_3$ and (b) $[(L(NIm^{Tol})_3)Fe_4S_4Cl][BPh_4]$ at 90 K. Black circles represent experimental data, solid lines are simulations. Simulation parameters: (a) Doublet 1: δ = 0.52 mm s^{-1}, ΔE_Q = 1.25 mm s^{-1}, Γ = 0.29 mm s^{-1}, rel. area = 0.5; Doublet 2: δ = 0.46 mm s^{-1}, ΔE_Q = 0.89 mm s^{-1}, Γ = 0.34 mm s^{-1}, relative area = 0.5. (b) Doublet 1: δ = 0.48 mm s^{-1}, ΔE_Q = 1.12 mm s^{-1}, Γ = 0.35 mm s^{-1}, rel. area = 0.75; Doublet 2: δ = 0.48 mm s^{-1}, ΔE_Q = 0.70 mm s^{-1}, Γ = 0.25 mm s^{-1}, relative area = 0.25. An alternate simulation for panel a is shown in Figure S25.

by modestly expanding or contracting its binding pocket. Our work demonstrates that this inherent challenge can be overcome by rationally modulating the sterics of the ligand, in this case using the steric bulk of the $L(NIm^{Tol})_3$ ligand to preclude formation of an $[Fe_6S_6]^{3+}$ cluster.

Another challenge in site-differentiated Fe−S cluster chemistry is modulating the steric environment of the unique Fe center(s). In 3:1 site-differentiated Fe_4S_4 clusters, the environment of the unique Fe center can only be controlled remotely by tuning the ligands to the other three Fe sites. In **12**, the orientation of the imidazolyl groups positions one of the *N*-tolyl groups on each donor arm in a manner so as to confer substantial steric protection to the unique Fe site (Figure 5). Moreover, the structure of **12** suggests further ways to tune the steric environment of the unique Fe site through simple modification of the imidazolyl ring substituents.

NIm donors have not been previously utilized in Fe−S cluster chemistry and are emerging as a useful ligand class in transition metal[50−52,76,77] and main group[78] chemistry. In complexes **11** and **12**, one lone pair of electrons on the donor N atom is used

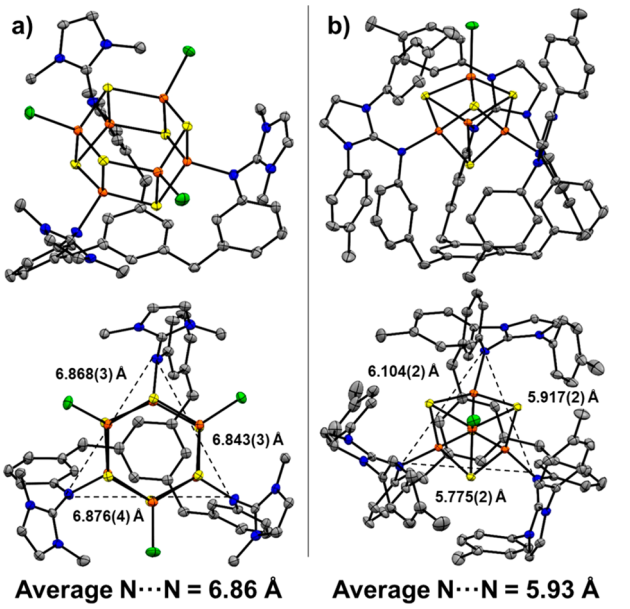

Figure 3. Thermal-ellipsoid (50%) plots of the solid-state structures of (a) $(L(NIm^{Me})_3)Fe_6S_6Cl_3$ and (b) $[(L(NIm^{Tol})_3)Fe_4S_4Cl][BPh_4]$. Orange, yellow, green, blue, and gray ellipsoids represent Fe, S, Cl, N, and C, respectively. H atoms, counterions, 4,5-phenyl substituents, and cocrystallized solvent molecules are omitted for clarity.

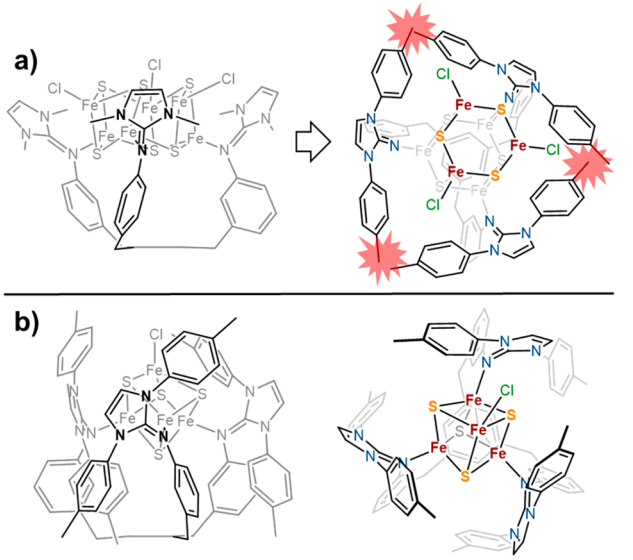

Figure 4. Simplified diagrams demonstrating (a) the upright positions of the imidazolyl substutents for $(L(NIm^{Me})_3)Fe_6S_6Cl_3$ and the resulting steric clash for the hypothetical molecule $(L(NIm^{Tol})_3)Fe_6S_6Cl_3$ and (b) tilt of the imidazolyl substituents for $[(L(NIm^{Tol})_3)Fe_4S_4Cl]^+$. Ph groups are omitted for clarity.

for σ bonding with Fe. The imidazolyl rings are oriented nearly perpendicularly to the remaining N lone pair, thereby minimizing delocalization into the imidazolyl π system and making the lone pair available for Fe−N π bonding.[47−49] As such, the NIm donors are best represented by their zwitterionic forms (Figure 6b).[79] We anticipate that the strong σ and π donor properties of NIm ligands will find further utility in Fe−S cluster chemistry.

DOI: 10.1021/acs.inorgchem.8b02684
Inorg. Chem. XXXX, XXX, XXX−XXX

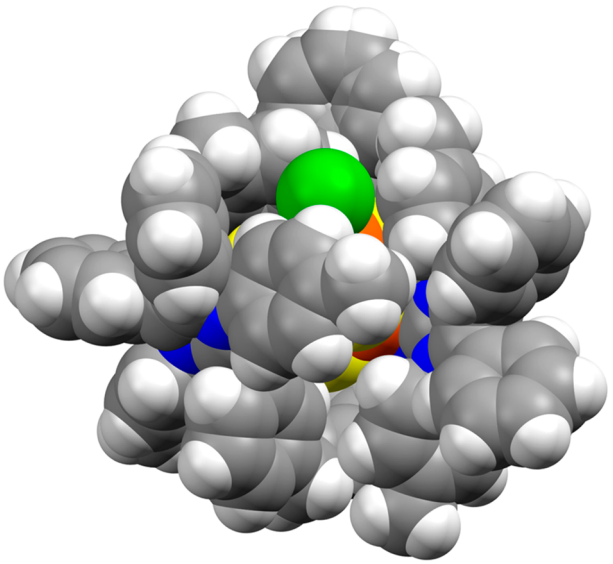

Figure 5. Space-filling model of the cationic portion of $[(L(NIm^{Tol})_3)Fe_4S_4Cl]^+$ (**12**).

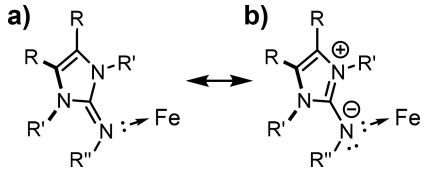

Figure 6. (a) Imino and (b) ylidic resonance contributers for imidazolin-2-imines bound to Fe.

CONCLUSIONS

In conclusion, tridentate ligands featuring imidazolin-2-imine donors with different steric properties may be prepared in synthetically useful quantities from a trianiline precursor. Metalation with the Fe−S cluster precursor $[Ph_4P]_2[Fe_4S_4Cl_4]$ provides clusters of different nuclearity. Short *N*-imidazolyl substituents such as methyl enable the preparation of Fe_6S_6 clusters whereas long *N*-imidazolyl substituents such as *p*-tolyl disfavor formation of Fe_6S_6 clusters and allow access to Fe_4S_4 clusters. Thus, through simple and rational modification of the steric profiles of the ligands, the nuclearity of the bound Fe−S clusters may be controlled with high selectivity.

ASSOCIATED CONTENT

Supporting Information

The Supporting Information is available free of charge on the ACS Publications website at DOI: 10.1021/acs.inorgchem.8b02684.

NMR spectra of new compounds, $^1H-^1H$ COSY spectra, UV−vis and EPR data for metal clusters, additional Mössbauer data, NMR spectra of reaction mixtures (PDF)

Accession Codes

CCDC 1868895−1868896 contain the supplementary crystallographic data for this paper. These data can be obtained free of charge via www.ccdc.cam.ac.uk/data_request/cif, or by emailing data_request@ccdc.cam.ac.uk, or by contacting The Cambridge Crystallographic Data Centre, 12 Union Road, Cambridge CB2 1EZ, UK; fax: +44 1223 336033.

AUTHOR INFORMATION

Corresponding Author

*E-mail: suess@mit.edu.

ORCID

Daniel L. M. Suess: 0000-0002-0916-1973

Funding

This work was supported in part by the MIT Skoltech Program.

Notes

The authors declare no competing financial interest.

ACKNOWLEDGMENTS

We thank Prof. Theodore Betley (Harvard University) for use of his Mössbauer spectrometer, Kevin Anderton (Harvard University) for assistance in acquiring the Mössbauer spectroscopic data, and Drs. Peter Müller and Charlene Tsay for assistance with X-ray crystallographic experiments.

REFERENCES

(1) Venkateswara Rao, P.; Holm, R. H. Synthetic Analogues of the Active Sites of Iron-Sulfur Proteins. *Chem. Rev.* **2004**, *104* (2), 527−559.

(2) Lee, S. C.; Holm, R. H. The Clusters of Nitrogenase: Synthetic Methodology in the Construction of Weak-Field Clusters. *Chem. Rev.* **2004**, *104* (2), 1135−1157.

(3) Lee, S. C.; Lo, W.; Holm, R. H. Developments in the Biomimetic Chemistry of Cubane-Type and Higher Nuclearity Iron-Sulfur Clusters. *Chem. Rev.* **2014**, *114* (7), 3579−3600.

(4) Roy, X.; Lee, C. H.; Crowther, A. C.; Schenck, C. L.; Besara, T.; Lalancette, R. A.; Siegrist, T.; Stephens, P. W.; Brus, L. E.; Kim, P.; Steigerwald, M. L.; Nuckolls, C. Nanoscale Atoms in Solid-State Chemistry. *Science* **2013**, *341* (6142), 157−160.

(5) Champsaur, A. M.; Velian, A.; Paley, D. W.; Choi, B.; Roy, X.; Steigerwald, M. L.; Nuckolls, C. Building Diatomic and Triatomic Superatom Molecules. *Nano Lett.* **2016**, *16* (8), 5273−5277.

(6) Zhong, X. J.; Lee, K.; Choi, B.; Meggiolaro, D.; Liu, F.; Nuckolls, C.; Pasupathy, A.; De Angelis, F.; Batail, P.; Roy, X.; Zhu, X. Y. Superatomic Two-Dimensional Semiconductor. *Nano Lett.* **2018**, *18* (2), 1483−1488.

(7) Champsaur, A. M.; Yu, J.; Roy, X.; Paley, D. W.; Steigerwald, M. L.; Nuckolls, C.; Bejger, C. M. Two-Dimensional Nanosheets from Redox-Active Superatoms. *ACS Cent. Sci.* **2017**, *3* (9), 1050−1055.

(8) Stiebritz, M. T.; Hiller, C. J.; Sickerman, N. S.; Lee, C. C.; Tanifuji, K.; Ohki, Y.; Hu, Y. Ambient Conversion of CO_2 to Hydrocarbons by Biogenic and Synthetic $[Fe_4S_4]$. *Clusters. Nat. Catal.* **2018**, *1*, 444−451.

(9) Inoue, H.; Shirai, M.; Haruki, E. Catalytic Function of the Fe_4S_4 Cluster in the Reduction of Aromatic Nitrocompounds with Tert-Butyl Thiol and Triethylamine. *J. Chem. Soc., Chem. Commun.* **1987**, No. 9, 674−675.

(10) Tezuka, M.; Yajima, T.; Tsuchiya, A.; Matsumoto, Y.; Uchida, Y.; Hidai, M. Electroreduction of Carbon-Dioxide Catalyzed by Iron Sulfur Clusters $[Fe_4S_4(SR)_4]^{2-}$. *J. Am. Chem. Soc.* **1982**, *104* (24), 6834−6836.

(11) Liu, J.; Kelley, M. S.; Wu, W.; Banerjee, A.; Douvalis, A. P.; Wu, J.; Zhang, Y.; Schatz, G. C.; Kanatzidis, M. G. Nitrogenase−Mimic Iron−Containing Chalcogels for Photochemical Reduction of Dinitrogen to Ammonia. *Proc. Natl. Acad. Sci. U. S. A.* **2016**, *113* (20), 5530−5535.

(12) Yuhas, B. D.; Smeigh, A. L.; Douvalis, A. P.; Wasielewski, M. R.; Kanatzidis, M. G. Photocatalytic Hydrogen Evolution from FeMoS-Based Biomimetic Chalcogels. *J. Am. Chem. Soc.* **2012**, *134* (25), 10353−10356.

(13) Yuhas, B. D.; Prasittichai, C.; Hupp, J. T.; Kanatzidis, M. G. Enhanced Electrocatalytic Reduction of CO_2 with Ternary Ni-Fe_4S_4 and Co-Fe_4S_4-Based Biomimetic Chalcogels. *J. Am. Chem. Soc.* **2011**, *133* (40), 15854−15857.

(14) Yuhas, B. D.; Smeigh, A. L.; Samuel, A. P.; Shim, Y.; Bag, S.; Douvalis, A. P.; Wasielewski, M. R.; Kanatzidis, M. G. Biomimetic

DOI: 10.1021/acs.inorgchem.8b02684
Inorg. Chem. XXXX, XXX, XXX−XXX

Multifunctional Porous Chalcogels as Solar Fuel Catalysts. *J. Am. Chem. Soc.* **2011**, *133* (19), 7252−7255.
(15) Shim, Y.; Yuhas, B. D.; Dyar, S. M.; Smeigh, A. L.; Douvalis, A. P.; Wasielewski, M. R.; Kanatzidis, M. G. Tunable Biomimetic Chalcogels with Fe_4S_4 Cores and $[Sn_nS_{2n+2}]^{4-}$ (n = 1, 2, 4) Building Blocks for Solar Fuel Catalysis. *J. Am. Chem. Soc.* **2013**, *135* (6), 2330−2337.
(16) Tanifuji, K.; Sickerman, N.; Lee, C. C.; Nagasawa, T.; Miyazaki, K.; Ohki, Y.; Tatsumi, K.; Hu, Y.; Ribbe, M. W. Structure and Reactivity of an Asymmetric Synthetic Mimic of Nitrogenase Cofactor. *Angew. Chem., Int. Ed.* **2016**, *55* (50), 15633−15636.
(17) Sickerman, N. S.; Tanifuji, K.; Lee, C. C.; Ohki, Y.; Tatsumi, K.; Ribbe, M. W.; Hu, Y. L. Reduction of C-1 Substrates to Hydrocarbons by the Homometallic Precursor and Synthetic Mimic of the Nitrogenase Cofactor. *J. Am. Chem. Soc.* **2017**, *139* (2), 603−606.
(18) Fontecave, M.; Ollagnier-de-Choudens, S. Iron-Sulfur Cluster Biosynthesis in Bacteria: Mechanisms of Cluster Assembly and Transfer. *Arch. Biochem. Biophys.* **2008**, *474* (2), 226−237.
(19) Bandyopadhyay, S.; Chandramouli, K.; Johnson, M. K. Iron-Sulfur Cluster Biosynthesis. *Biochem. Soc. Trans.* **2008**, *36*, 1112−1119.
(20) Black, K. A.; Dos Santos, P. C. Shared-Intermediates in the Biosynthesis of Thio-Cofactors: Mechanism and Functions of Cysteine Desulfurases and Sulfur Acceptors. *Biochim. Biophys. Acta, Mol. Cell Res.* **2015**, *1853* (6), 1470−1480.
(21) Dance, I.; Fisher, K. Metal Chalcogenide Cluster Chemistry. *Prog. Inorg. Chem.* **2007**, *41*, 637−803.
(22) Holm, R. H.; Lo, W. Structural Conversions of Synthetic and Protein-Bound Iron-Sulfur Clusters. *Chem. Rev.* **2016**, *116* (22), 13685−13713.
(23) Wong, G. B.; Bobrik, M. A.; Holm, R. H. Inorganic Derivatives of Iron Sulfide Thiolate Dimers and Tetramers - Synthesis and Properties of Halide Series $[Fe_2S_2X_4]^{2-}$ and $[Fe_4S_4X_4]^{2-}$ (X = Cl, Br, I). *Inorg. Chem.* **1978**, *17* (3), 578−584.
(24) Coucouvanis, D.; Kanatzidis, M.; Simhon, E.; Baenziger, N. C. Synthesis, Molecular-Structure, and Reactions of Bis-(Tetraphenylphosphonium) Hexakis(μ-Thiophenolato)-Tetrachlorotetraferrate(II), $(Ph_4P)_2[Fe_4(SPh)_6Cl_4]$ - Its Reactions with Dibenzyl Trisulfide and the Synthesis of the $[Fe_4S_4Cl_4]^{2-}$ and $[Fe_4S_4Cl_2(SC_6H_5)_2]^{2-}$ Cubane−Type Clusters. *J. Am. Chem. Soc.* **1982**, *104* (7), 1874−1882.
(25) Appelt, R.; Vahrenkamp, H.; Darensbourg, D. J.; Phelps, A. L.; Adams, M. J. Cyanometal-Substituted Derivatives of the Fe_4S_4 Cluster Core. *Inorg. Synth.* **2004**, *34*, 161−166.
(26) Kanatzidis, M. G.; Salifoglou, A.; Coucouvanis, D. A New Fe/S Cluster with the $(Fe_6S_6)^{3+}$ Prismatic Core and Para-Methylphenolate Terminal Ligands - the Synthesis, Structure, and Properties of $(Et_4N)_3Fe_6S_6(OC_6H_4\text{-}p\text{-}CH_3)_6$. *J. Am. Chem. Soc.* **1985**, *107* (11), 3358−3360.
(27) Kanatzidis, M. G.; Dunham, W. R.; Hagen, W. R.; Coucouvanis, D. A New Iron Sulfide Cluster Containing the Prismane $[Fe_6(\mu\text{-}S)_6]^{3+}$ Core - Synthesis, Structure, and Properties of $[Et_4N]_3[Fe_6S_6Cl_6]$. *J. Chem. Soc., Chem. Commun.* **1984**, *0* (6), 356−358.
(28) Kanatzidis, M. G.; Hagen, W. R.; Dunham, W. R.; Lester, R. K.; Coucouvanis, D. Metastable Fe/S Clusters. The Synthesis, Electronic Structure, and Transformations of the $[Fe_6S_6L_6]^{3-}$ Clusters (L = Cl^-, Br, I^-, RS^-, RO^-) and the Structure of $[(C_2H_5)_4N]_3[Fe_6S_6Cl_6]$. *J. Am. Chem. Soc.* **1985**, *107* (4), 953−961.
(29) Coucouvanis, D.; Kanatzidis, M. G.; Dunham, W. R.; Hagen, W. R. Oxidative Transformation of the $[Fe_4S_4X_4]^{2-}$ Cubanes to the $[Fe_6S_6X_6]^{2-}$ Prismane Clusters (X = Cl, Br) - the Crystal and Molecular-Structure of $[(C_6H_5)_4P]_2Fe_6S_6Cl_6$. *J. Am. Chem. Soc.* **1984**, *106* (25), 7998−7999.
(30) Goh, C.; Segal, B. M.; Huang, J. S.; Long, J. R.; Holm, R. H. Polycubane Clusters: Synthesis of $[Fe_4S_4(PR_3)_4]^{(1+,0)}$ (R = Bu^tCy, Pr^i) and $[Fe_4S_4]^0$ Core Aggregation upon Loss of Phosphine. *J. Am. Chem. Soc.* **1996**, *118* (47), 11844−11853.
(31) Stack, T. D. P.; Holm, R. H. Subsite-Specific Functionalization of the $[4Fe\text{-}4S]^{2+}$ Analog of Iron Sulfur Protein Clusters. *J. Am. Chem. Soc.* **1987**, *109* (8), 2546−2547.
(32) Stack, T. D. P.; Holm, R. H. Subsite-Differentiated Analogs of Biological $[4Fe\text{-}4S]^{2+}$ Clusters - Synthesis, Solution and Solid-State Structures, and Subsite-Specific Reactions. *J. Am. Chem. Soc.* **1988**, *110* (8), 2484−2494.
(33) Zhou, J.; Hu, Z. G.; Munck, E.; Holm, R. H. The Cuboidal Fe_3S_4 Cluster: Synthesis, Stability, and Geometric and Electronic Structures in a Non-Protein Environment. *J. Am. Chem. Soc.* **1996**, *118* (8), 1966−1980.
(34) Hagen, K. S.; Watson, A. D.; Holm, R. H. Synthetic Routes to $Fe_2S_2Fe_3S_4Fe_4S_4$ and Fe_6S_9 Clusters from the Common Precursor $[Fe(SC_2H_5)_4]^{2-}$ - Structures and Properties of $[Fe_3S_4(SR)_4]^{3-}$ and $[Fe_6S_9(SC_2H_5)_2]^{4-}$ Examples of the Newest Types of Fe-S-SR Clusters. *J. Am. Chem. Soc.* **1983**, *105* (12), 3905−3913.
(35) Hagen, K. S.; Holm, R. H. Systematic Iron(II)-Thiolate Chemistry - Synthetic Entry to Trinuclear Complexes. *J. Am. Chem. Soc.* **1982**, *104* (20), 5496−5497.
(36) Zhao, Q. L.; Betley, T. A. Synthesis and Redox Properties of Triiron Complexes Featuring Strong Fe-Fe Interactions. *Angew. Chem., Int. Ed.* **2011**, *50* (3), 709−712.
(37) Zhao, Q. L.; Harris, T. D.; Betley, T. A. $[(^{H}L)_2Fe_6(NCMe)_m]^n$ (m = 0, 2, 4, 6; n = − 1, 0, 1, 2, 3, 4, 6): An Electron-Transfer Series Featuring Octahedral Fe-6 Clusters Supported by a Hexaamide Ligand Platform. *J. Am. Chem. Soc.* **2011**, *133* (21), 8293−8306.
(38) Sanchez, R. H.; Willis, A. M.; Zheng, S. L.; Betley, T. A. Synthesis of Well-Defined Bicapped Octahedral Iron Clusters $[(^{tren}L)_2Fe_8(PMe_2Ph)_2]^n$ (n = 0, −1). *Angew. Chem., Int. Ed.* **2015**, *54* (41), 12009−12013.
(39) Lee, Y.; Jeon, I. R.; Abboud, K. A.; Garcia-Serres, R.; Shearer, J.; Murray, L. J. A $[3Fe\text{-}3S]^{3+}$ Cluster with Exclusively μ−Sulfide Donors. *Chem. Commun.* **2016**, *52* (6), 1174−1177.
(40) Murray, L. J.; Weare, W. W.; Shearer, J.; Mitchell, A. D.; Abboud, K. A. Isolation of a (Dinitrogen)Tricopper(I) Complex. *J. Am. Chem. Soc.* **2014**, *136* (39), 13502−13505.
(41) Lee, Y.; Sloane, F. T.; Blondin, G.; Abboud, K. A.; Garcia-Serres, R.; Murray, L. J. Dinitrogen Activation Upon Reduction of a Triiron(II) Complex. *Angew. Chem., Int. Ed.* **2015**, *54* (5), 1499−1503.
(42) Guillet, G. L.; Sloane, F. T.; Ermert, D. M.; Calkins, M. W.; Peprah, M. K.; Knowles, E. S.; Cizmar, E.; Abboud, K. A.; Meisel, M. W.; Murray, L. J. Preorganized Assembly of Three Iron(II) or Manganese(II) Beta−Diketiminate Complexes Using a Cyclophane Ligand. *Chem. Commun.* **2013**, *49* (59), 6635−6637.
(43) Tsui, E. Y.; Kanady, J. S.; Agapie, T. Synthetic Cluster Models of Biological and Heterogeneous Manganese Catalysts for O_2 Evolution. *Inorg. Chem.* **2013**, *52* (24), 13833−13848.
(44) Tsui, E. Y.; Tran, R.; Yano, J.; Agapie, T. Redox-Inactive Metals Modulate the Reduction Potential in Heterometallic Manganese−Oxido Clusters. *Nat. Chem.* **2013**, *5* (4), 293−299.
(45) Kanady, J. S.; Tsui, E. Y.; Day, M. W.; Agapie, T. A Synthetic Model of the Mn_3Ca Subsite of the Oxygen-Evolving Complex in Photosystem II. *Science* **2011**, *333* (6043), 733−736.
(46) Kunetskiy, R. A.; Polyakova, S. M.; Vavrik, J.; Cisarova, I.; Saame, J.; Nerut, E. R.; Koppel, I.; Koppel, I. A.; Kutt, A.; Leito, I.; Lyapkalo, I. M. A New Class of Organosuperbases, N-Alkyl- and N-Aryl-1,3-dialkyl-4,5-dimethylimidazol-2-ylidene Amines: Synthesis, Structure, pK-(BH^+) Measurements, and Properties. *Chem. - Eur. J.* **2012**, *18* (12), 3621−3630.
(47) Petrovic, D.; Gloge, T.; Bannenberg, T.; Hrib, C. G.; Randoll, S.; Jones, P. G.; Tamm, M. Synthesis and Reactivity of 16-Electron Pentamethylcyclopentadienyl-Ruthenium(II) Complexes with Bis-(imidazolin-2-imine) Ligands. *Eur. J. Inorg. Chem.* **2007**, *2007* (22), 3472−3475.
(48) Petrovic, D.; Hill, L. M. R.; Jones, P. G.; Tolman, W. B.; Tamm, M. Synthesis and Reactivity of Copper(I) Complexes with an Ethylene-Bridged Bis(imidazolin-2-imine) Ligand. *Dalton Trans.* **2008**, No. 7, 887−894.
(49) Herres-Pawlis, S.; Florke, U.; Henkel, G. Tuning of Copper(I)-Dioxygen Reactivity by Bis(guanidine) Ligands. *Eur. J. Inorg. Chem.* **2005**, *2005* (19), 3815−3824.

DOI: 10.1021/acs.inorgchem.8b02684
Inorg. Chem. XXXX, XXX, XXX−XXX

(50) Gloge, T.; Petrovic, D.; Hrib, C. G.; Daniliuc, C.; Herdtweck, E.; Jones, P. G.; Tamm, M. Synthesis and Structural Characterisation of an Isomorphous Series of Bis(imidazolin-2-imine) Metal Dichlorides Containing the First Row Transition Metals Mn, Fe, Co, Ni, Cu and Zn. *Z. Anorg. Allg. Chem.* **2010**, *636* (13−14), 2303−2308.
(51) Filimon, S. A.; Petrovic, D.; Volbeda, J.; Bannenberg, T.; Jones, P. G.; Freiherr von Richthofen, C.-G.; Glaser, T.; Tamm, M. 3d Metal Complexes Supported by a Bis(imidazolin-2-imino)pyridine Pincer Ligand - Synthesis, Structural Characterisation, and Magnetic Properties. *Eur. J. Inorg. Chem.* **2014**, *2014* (35), 5997−6012.
(52) Jess, K.; Baabe, D.; Freytag, M.; Jones, P. G.; Tamm, M. Transition-Metal Complexes with Ferrocene-Bridged Bis-(imidazolin-2-imine) and Bis(diaminocyclopropenimine) Ligands. *Eur. J. Inorg. Chem.* **2017**, *2017* (34), 412−423.
(53) Schubert, E. M. Utilizing the Evans Method with a Superconducting NMR Spectrometer in the Undergraduate Laboratory. *J. Chem. Educ.* **1992**, *69* (1), 62−62.
(54) Bain, G. A.; Berry, J. F. Diamagnetic corrections and Pascal's constants. *J. Chem. Educ.* **2008**, *85* (4), 532−536.
(55) Prisecaru, I. WMOSS4 Mössbauer Spectral Analysis Software, 2016., www.wmoss.org.
(56) *SADABS*, v2014/5; Bruker AXS Inc.: Madison, WI, 2001.
(57) Sheldrick, G. M. SHELXT - Integrated Space-Group and Crystal-Structure Determination. *Acta Crystallogr., Sect. A: Found. Adv.* **2015**, *71*, 3−8.
(58) Sheldrick, G. M. Crystal Structure Refinement with SHELXL. *Acta Crystallogr., Sect. C: Struct. Chem.* **2015**, *71*, 3−8.
(59) Kim, Y. B.; Kim, C. S.; Lee, C. K. Condensation-Reactions of Aryl Acyloins with Ureas in Ethylene-Glycol. *J. Heterocycl. Chem.* **1994**, *31* (6), 1653−1656.
(60) Mehrotra, K. N.; Singh, G. New Synthetic Method for 1,3,4,5-Tetraaryl-2-thioxo-2,3-dihydroimidazoles(or 1,3,4,5-tetraaryl-2-oxo)-2,3-dihydroimidazoles. *Synthesis* **1980**, *1980* (12), 1001−1004.
(61) Safir Filho, M.; Martin, A. R.; Benhida, R. Assessment of New Triplet Forming Artificial Nucleobases as RNA Ligands Directed Towards HCV IRES IIId Loop. *Bioorg. Med. Chem. Lett.* **2017**, *27* (8), 1780−1783.
(62) Pigge, F. C.; Ghasedi, F.; Zheng, Z. M.; Rath, N. P.; Nichols, G.; Chickos, J. S. Structural Characterization of Crystalline Inclusion Complexes Formed from 1,3,5-Triaroylbenzene Derivatives - a New Family of Inclusion Hosts. *J. Chem. Soc. Perkin Trans. 2* **2000**, No. 12, 2458−2464.
(63) Walsdorff, C.; Saak, W.; Pohl, S. A New Preorganized Tridentate Ligand Bearing Three Indolethiolate Groups. Preparation of 3:1 Subsite-Differentiated Fe_4S_4 Clusters. *J. Chem. Soc., Dalton Trans.* **1997**, No. 11, 1857−1861.
(64) Terada, T.; Wakimoto, T.; Nakamura, T.; Hirabayashi, K.; Tanaka, K.; Li, J.; Matsumoto, T.; Tatsumi, K. Tridentate Thiolate Ligands: Application to the Synthesis of the Site-Differentiated [4Fe-4S] Cluster having a Hydrosulfide Ligand at the Unique Iron Center. *Chem. - Asian J.* **2012**, *7* (5), 920−929.
(65) Terada, T.; Hirabayashi, K.; Liu, D.; Nakamura, T.; Wakimoto, T.; Matsumoto, T.; Tatsumi, K. [3:1] Site-Differentiated [4Fe-4S] Clusters Having One Carboxylate and Three Thiolates. *Inorg. Chem.* **2013**, *52* (20), 11997−12004.
(66) Kanatzidis, M. G.; Salifoglou, A.; Coucouvanis, D. Chemistry of $[Fe_6S_6]^{3+}$ Prismatic Cages - Synthesis, Structural Characterization, and Electronic−Structures of the $[Et_4N]_3[Fe_6S_6Cl_6]$ Clusters (L = p-$CH_3C_6H_4O^-Br^-$). *Inorg. Chem.* **1986**, *25* (14), 2460−2468.
(67) Groom, C. R.; Bruno, I. J.; Lightfoot, M. P.; Ward, S. C. The Cambridge Structural Database. *Acta Crystallogr., Sect. B: Struct. Sci., Cryst. Eng. Mater.* **2016**, *72*, 171−179.
(68) Papaefthymiou, G. C.; Laskowski, E. J.; Frotapessoa, S.; Frankel, R. B.; Holm, R. H. Anti-Ferromagnetic Exchange Interactions in $[Fe_4S_4(SR)_4]^{2-,3-}$ Clusters. *Inorg. Chem.* **1982**, *21* (5), 1723−1728.
(69) Reynolds, J. G.; Laskowski, E. J.; Holm, R. H. Proton Magnetic-Resonance Properties of Tetranuclear Clusters $[Fe_4S_4(SR)_4]^{3-}$ Analogs of 4-Fe Sites of Reduced Ferredoxins. *J. Am. Chem. Soc.* **1978**, *100* (17), 5315−5322.
(70) Ciurli, S.; Carrie, M.; Weigel, J. A.; Carney, M. J.; Stack, T. D. P.; Papaefthymiou, G. C.; Holm, R. H. Subsite−Differentiated Analogs of Native $[4Fe\text{-}4S]^{2+}$ Clusters − Preparation of Clusters with 5-Coordinate and 6-Coordinate Subsites and Modulation of Redox Potentials and Charge-Distributions. *J. Am. Chem. Soc.* **1990**, *112* (7), 2654−2664.
(71) Evans, D. J.; Garcia, G.; Leigh, G. J.; Newton, M. S.; Santana, M. D. Triazacyclane-Based Trithiols and Their Use in the Preparation of Site-Differentiated Iron Sulfur Clusters. *J. Chem. Soc., Dalton Trans.* **1992**, No. 22, 3229−3234.
(72) Beinert, H.; Holm, R. H.; Munck, E. Iron-Sulfur Clusters: Nature's Modular, Multipurpose Structures. *Science* **1997**, *277* (5326), 653−659.
(73) Bominaar, E. L.; Hu, Z. G.; Munck, E.; Girerd, J. J.; Borshch, S. A. Double Exchange and Vibronic Coupling in Mixed-Valence Systems - Electronic-Structure of Exchange-Coupled Siroheme - $[Fe_4S_4]^{2+}$ Chromophore in Oxidized Escherichia-Coli Sulfite Reductase. *J. Am. Chem. Soc.* **1995**, *117* (26), 6976−6989.
(74) Silver, J.; Fern, G. R.; Miller, J. R.; McCammon, C. A.; Evans, D. J.; Leigh, G. J. Effects of Temperature and Pressure on the Mössbauer Spectra of Models for the $[4Fe_4]^{2+}$ Clusters of Iron-Sulfur Proteins and the Structure of $[PPh_4]_2[Fe_4S_4(SCH_2CO_2C_2H_5)_4]$. *Inorg. Chem.* **1999**, *38* (19), 4256−4261.
(75) Holm, R. H.; Averill, B. A.; Herskovitz, T.; Frankel, R. B.; Gray, H. B.; Siiman, O.; Grunthaner, F. J. Equivalence of Metal Centers in Iron-Sulfur Protein Active-Site Analogs $[Fe_4S_4(SR)_4]^{2-}$. *J. Am. Chem. Soc.* **1974**, *96* (8), 2644−2646.
(76) Bruns, H.; Patil, M.; Carreras, J.; Vazquez, A.; Thiel, W.; Goddard, R.; Alcarazo, M. Synthesis and Coordination Properties of Nitrogen(I)-Based Ligands. *Angew. Chem., Int. Ed.* **2010**, *49* (21), 3680−3683.
(77) Li, S. H.; Lin, Y. J.; Cao, J. G.; Zhang, S. B. Guanidine/$Pd(OAc)_2$-Catalyzed Room Temperature Suzuki Cross-Coupling Reaction in Aqueous Media under Aerobic Conditions. *J. Org. Chem.* **2007**, *72* (11), 4067−4072.
(78) Franz, D.; Irran, E.; Inoue, S. Isolation of a Three-Coordinate Boron Cation with a Boron-Sulfur Double Bond. *Angew. Chem., Int. Ed.* **2014**, *53* (51), 14264−14268.
(79) Tamm, M.; Petrovic, D.; Randoll, S.; Beer, S.; Bannenberg, T.; Jones, P. G.; Grunenberg, O. Structural and Theoretical Investigation of 2-Iminoimidazolines - Carbene Analogues of Iminophosphoranes. *Org. Biomol. Chem.* **2007**, *5* (3), 523−530.

DOI: 10.1021/acs.inorgchem.8b02684
Inorg. Chem. XXXX, XXX, XXX−XXX